available at www.sciencedirect.com

ScienceDirect

journal homepage: www.elsevier.com/locate/ecolmodel

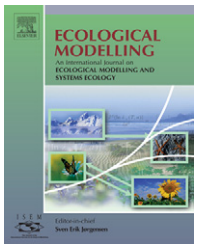

A simple net ecosystem productivity model for gap filling of tower-based fluxes: An extension of Landsberg's equation with modifications to the light interception term

Zisheng Xing[a], *Charles P.-A. Bourque*[a,*], *Fanrui Meng*[a], *Tianshan Zha*[b], *Roger M. Cox*[c], *D. Edwin Swift*[c]

[a] *Faculty of Forestry & Environmental Management, University of New Brunswick, Fredericton, New Brunswick, Canada E3B 6C2*
[b] *Climate Research Branch, Environment Canada, 11 Innovation RD, Saskatoon, Saskatchewan, Canada S7N 3H5*
[c] *Natural Resources Canada, Canadian Forest Service, Atlantic Forestry Centre, P.O. Box 4000, Fredericton, New Brunswick, Canada E3B 5P7*

ARTICLE INFO

Article history:
Received 13 April 2006
Received in revised form
12 March 2007
Accepted 28 March 2007
Published on line 25 May 2007

Keywords:
Environmental conditions
Fluxnet-Canada
Forest ecosystem
Gap filling
Landsberg's equation
Light interception
Multiple-layer canopy
Net ecosystem productivity
Two big-leaf model

ABSTRACT

Net ecosystem productivity (NEP) is a key ecological variable in forestry and carbon sequestration sciences. Advances in eddy-covariance instrumentation in recent years have improved the accuracy to which productivity in ecosystems can be measured. However, equipment failure, power outages, system maintenance shutdowns, and inclement weather frequently introduce gaps in the measurement data stream, which can reduce the integrity, usefulness, and interpretation of the data. To compensate for these limitations, a simple NEP model with few automatically adjustable parameters is developed to improve gap filling of discontinuous time series. Initial model formulation and parameter-value determination are founded on 2004 growing-season NEP measurements collected at eight Fluxnet-Canada (FCRN) stations (i.e., eight ecosystems) from across Canada's southern commercial forest zone. A preliminary inter-equation comparison of three commonly used flux equations, all with photosynthetically active radiation (PAR) as the independent variable, revealed that the three equations provided similar mean description of NEP. In this paper, we use Landsberg's equation [Landsberg, J.J., 1977. Some useful equations for biological studies. Exp. Agric. 13, 272–286] in modelling NEP. Initial parameter values of the Landsberg's equation were shown to depend on forest species composition, stand age, and existing site conditions. Further analysis indicated that on average for a 9-day period for the Atlantic Maritime balsam fir site in New Brunswick, Landsberg's equation represented mean NEP very well for cloudy days, but performed poorly when light conditions deviated from average conditions. We hypothesized that variation in the level of diffuse and direct radiation contributed to differences in light response. As Landsberg's equation does not explicitly address (i) light quality, i.e., level of diffuse to direct illumination, and (ii) vertical canopy structure, a simple NEP model combining Landsberg's equation with a two big-leaf (sunlit versus shade leaf model concept) and multiple-layer canopy light transmission formulation was developed for modelling the day-to-day variation in NEP and for gap filling. Results from these enhancements captured more of the NEP peaks (coefficient of determination, $r^2 = 0.70$) than were previously modelled with

* *Corresponding author*. Tel.: +1 506 453 4930; fax: +1 506 453 3538.
E-mail address: cbourque@unb.ca (C.P.-A. Bourque).

doi:10.1016/j.ecolmodel.2007.03.031

the unaltered form of Landsberg's equation ($r^2 = 0.63$). Model sensitivity analysis suggested partitioning the canopy in four canopy layers provided the best overall improvement in NEP calculations; beyond four layers, model improvement was minor.

1. Introduction

The Fluxnet-Canada Research Network (FCRN) was established in 2002 to examine how management practices, natural disturbance, and climate variability influence carbon (C) cycling in forest and peatland ecosystems in Canada (Coursolle et al., 2006). Although many studies have been performed in recent years on the resulting information to investigate daily, seasonal, and annual patterns in net ecosystem exchange (NEE or negative of net ecosystem productivity, NEP), and environmental flux controls (Arain and Restrepo-Cope, 2005; Amiro et al., 2006), preparation and interpretation of the data have been significantly encumbered by the presence of gaps in the data. These gaps are typically created as a result of inclement weather (e.g., ice accretion on sensors, lighting strikes, sensor surface wetting), system maintenance shutdowns, and equipment failure (Hui et al., 2004), and introduce a level of diminished quality to the dataset. For this reason, gap filling is a necessary task in improving the quality and usefulness of the flux data. Badly filled gaps introduce error in the data, and make interpretation of the data difficult.

For effective gap filling, the method employed should: (i) be easy to implement; (ii) capture prominent features of the modelled system and address interactions among the most important environment controls; (iii) have limited number of model parameters for auto-parameterization (parameter optimization), and (iv) have few inter-correlated parameters so that model parameterization is internally consistent. Currently, data gaps less than an hour can be effectively filled by simple linear interpolation. Gaps lasting longer than a few days, however, require biophysically based methods to account for the day-to-day and hour-to-hour variation in environmental controls.

Currently, gaps are filled by one of the following methods: (i) *Lookup tables* (*LT*) use a randomly or systematically chosen value from individual observations that has similar values on other variables (Falge et al., 2001a,b; Greco and Baldocchi, 1996); (ii) *Non-linear regression* (*NLR*) is used to estimate missing values with mathematical expressions generated by regressing dependent variables against explanatory variables; (iii) *Artificial neural networks* (*ANN*) generate predictive models (networks) of simple processing elements (i.e., neurons) by iterative learning (Aubinet et al., 2000); (iv) *Multiple imputation* (*MI*) provides a set of values through standard statistical techniques (Hui et al., 2004), and (v) *Ecosystem models* (*EM*).

Generally, statistical methods (e.g., MI) fail to produce ecologically meaningful predictions as they fail to address the inherent relationships among the ecological state variables. Some methods lack the flexibility for application beyond the conditions used in their development (e.g., LT's). ANN's have the ability to consider many controlling variables in model formulation and generally perform very well with highly non-linear relationships between input and output (target) variables. The structures generated, however, fail to provide meaningful explanation of the data and relationships among state variables. As a simple black-box approach to gap filling, the method is quite effective. However, ANN structures are prone to over-fitting (over-generalization), imparting some level of uncertainty to gap-filled values. Ecosystem models like C-Class, BEPS, and *ecosys* described in Verseghy et al. (1991), Liu et al. (1997), and Grant et al. (2005) can be used for gap filling. However, because of their many inter-correlated parameters, auto-parameterization of such models using numerical methods, such as the Levenberg–Marquardt or Simplex methods is normally difficult because of internal inconsistencies and problems associated with solution divergence. Typically, parameterization of such models is done by trial and error and is very time consuming. As a general rule, as the number of model parameters increase, the statistical stability of the model decreases. An appropriate model for gap filling should technically balance relevant ecological detail with the number of inter-correlated, redundant parameters in model formulation.

Carbon sequestration by forest ecosystems (i.e., NEP) results from the combined interactions between plant species, soil conditions, climate, disturbance regimes, and meteorological and micrometeorological factors (Bhatti et al., 2002; Taylor and MacLean, 2005). Among the many micro-meteorological factors, available photosynthetically active radiation (PAR) plays a predominant role in defining NEP at the leaf to stand level (Coursolle et al., 2006) and, as a consequence, is often the focus in ecological studies (e.g., Anderson et al., 2000; Chen et al., 2002; Arain and Restrepo-Cope, 2005).

Several PAR-based formulations to model NEP and gross ecosystem productivity (GEP = NEP + R_d, where R_d is ecosystem respiration) are currently being used to either gap fill discontinuous datasets or for performing ecosystem productivity analyses. For example, FCRN recommends the use of

$$\mathrm{NEP} = \frac{\alpha P_x \mathrm{PAR}}{\alpha \mathrm{PAR} + P_x} - R_d \quad (1)$$

for gap filling. In Eq. (1), P_x is the GEP at the point of light saturation, PAR the incident PAR, and α is the quantum yield, an equation coefficient. The same expression was used in (Amiro et al., 2006) in the analysis of forest ecosystem productivity in Saskatchewan. Hollinger et al. (1998) used

$$\mathrm{NEP} = \frac{a\mathrm{PAR}}{b + \mathrm{PAR}} - R_d \quad (2)$$

to estimate NEP at the Howland flux site, Maine, USA, where a and b are equation parameters.

Landsberg's equation (1977) (**Model 1** hereafter, for convenience of discussion), is expressed as

$$\mathrm{NEP} = \mathrm{NEP}_{\max} \cdot (1 - \exp(-\alpha(\mathrm{PAR} - \Gamma))) \quad (3)$$

where NEP_{max} is maximum NEP ($\mu mol\ CO_2\ m^{-2}\ s^{-1}$), α the quantum efficiency parameter [$mol\ CO_2\ (mol\ PAR)^{-1}$; a shape factor] and Γ is the light compensation point ($\mu mol\ PAR\ m^{-2}\ s^{-1}$); when $PAR = \Gamma$, respiration (R_d) = photosynthesis (NEP = 0), and when $0 < PAR \leq \Gamma$, respiration (R_d) > photosynthesis, and NEP < 0. The equation has been widely used to (i) investigate ecosystem productivity in diverse ecosystems across Canada (Coursolle et al., 2006), (ii) analyze local-scale environmental controls on forest growth (Bourque et al., 2006), and (iii) analyze influences of forest age on NEP (Chen et al., 2002). In general, expressing NEP as function of PAR with Landsberg's equation (1977) can explain about 50–70% of the variation in NEP (Mäkelä et al., 1996; Chen et al., 2002; Bourque et al., 2006; Coursolle et al., 2006).

The two components of PAR (i.e., diffuse and direct PAR) have been found to promote different growth response in plants, and, as a result, separating the two light components is necessary to model global primary production (Gu et al., 2002) because diffuse radiation (i) is more efficiently used by plants; (ii) rarely reaches saturation levels; (iii) increases with an increase in radiation level; and (iv) influences on plant growth is modified by other environmental factors [e.g., water vapor pressure deficit (VPD), air temperature] during certain times of the day. In general, error in individual half-hourly prediction-to-measurement values of NEP has been shown to be as high as 300% when these simple PAR-based relationships were used. For instance, when Chen et al. (2002) used Landsberg's equation to investigate the variation of NEP with stand age in Douglas fir [*Pseudotsuga menziesii* (Mirb.) Franco] forests in the United States, it was found that NEP varied strongly with changes in PAR and above canopy VPD. It was concluded that Landsberg's equation underestimated NEP when VPD was low, and overestimated NEP when VPD was high.

Description of canopy light transmission in complex canopies can potentially lead to the development of complicated models. Increasing model complexity may increase model accuracy, but it does so at the expense of model stability.

Our objectives in this paper are (i) to select an appropriate equation for predicting the mean variation in NEP as a function of PAR; (ii) to fit the selected equation to NEP values measured over eight different forest ecosystems across Canada in order to evaluate the equation's suitability, limitations, and range of parameter values in the prediction of NEP; (iii) to develop a refined version of Landsberg's equation incorporating improvements to the way light interception (transmission) is addressed in the equation, and (iv) to evaluate the newly developed model against data from the Atlantic Maritime balsam fir [*Abies Balsamea* (L.) Mill.; BF] forest site in New Brunswick (NB), Canada.

2. Materials and methods

2.1. Study sites

The research sites involved in this study include five forest types along an east–west transect from NB to Vancouver Island, British Columbia (BC), Canada (Table 1; Fig. 1), including a balsam fir forest in west–central NB (NB_BF), one old mixed hardwood (OMW) and two white pine plantation forests (*Pinus*

Table 1 – Site description

Site	Species code[a]	Location (latitude N°, longitude W°)	Elevation (m)	Stand origin[b]	Age	Canopy height[c]	Dominant species[d]	LAI[e]	EC height[f]	Sonic anemometer[g]	IRGA[h]
NB_BF	BF	45.519, 67.100	341	H/N	36	14	BF	8.4	18.5	CSAT3	LI-7000
QC_OBS	BS	49.692, 74.342	393	F/N	100	14	BS, JP	4	25	CSAT3	LI-7500
ON_OMW	MW	48.217, 82.156	341	F/H/N	75		TA, WB, WS, RS, BF	4.1	41	CSAT3	LI-7500
ON_WPP39	WP	42.712, 80.357	184	F/H/P	65	22	WP	6.5	28	CSAT3	LI-7000
ON_WPP74	WP	42.709, 80.348	184	F/H/P	30	12	WP	4.5	18	CSAT3	LI-7500
SK_OA	OA	53.629, 106.2	601	F/N	84	20	TA	2.1	39	Gill R3	LI-6262
SK_OBS	BS	53.987, 105.117	629	F/N	123	11	BS	3.8	25	Gill R3	LI-6262
BC_DF	DF	49.905, 125.366	300	H/P	54	33	DF	7.3	43	Gill R3	LI-7000

[a] Tree species: BF: balsam fir; OBS: old black spruce; OMW: old mixedwood; WP: white pine; OA: old aspen; DF: Douglas fir.
[b] H/N: harvested/natural regeneration; F/N: fire/natural regeneration; F/H/P: fire/harvested/planted; H/P: harvested/planted.
[c] Height (m).
[d] JP: jack pine; TA: trembling aspen; WS: white spruce; RS: red spruce; WB: white birch.
[e] LAI: Leaf area index (m^2 leaf m^{-2} ground), data in this column are based on results from Chen et al. (2006).
[f] EC equipment installation height (m).
[g] CSAT3: Campbell Scientific, Logan, UT, USA; Gill R2, Gill R3: Gill Instruments Ltd., Lymington, Hampshire, UK.
[h] IRGA, Infrared gas analyzer; LI-7500 (open-path), LI-6262 (closed-path), LI-7000 (closed-path): LI-COR Inc., Lincoln, NE, USA.

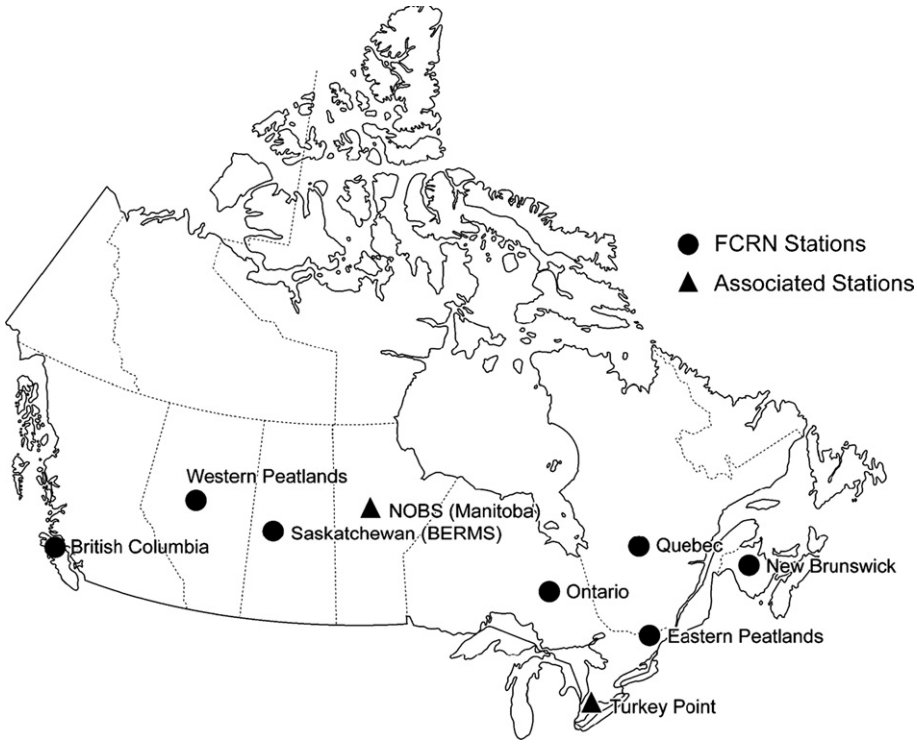

Fig. 1 – FCRN-site locations along an east–west transect across Canada's southern commercial forest zone (site descriptions are provided in Table 1; map of Canada and site locations are taken from Coursolle et al., 2006). Eight sites of interest for parameter value definition include the New Brunswick (NB_BF; balsam fir), Quebec (QC_OBS; old black spruce), Ontario (ON_OMW, ON_WPP39, and ON_WPP74; old mixedwood and white pine plantations), Saskatchewan (SK_OA, SK_OBS; old aspen and black spruce), and British Columbia (BC_DF; Douglas fir) sites.

strobus L.; WP) in Ontario (ON_OMW, ON_WPP39, ON_WPP74; number at the end of the site name provides the year of stand initiation, i.e., 1939 and 1974, respectively), two old black spruce [*Picea mariana* (Mill.) BSP; BS] forests in Quebec (QC_OBS) and Saskatchewan (SK_OBS), an old aspen (*Populus tremuloides* Michx.; OA) forest in Saskatchewan (SK_OA), and a Douglas fir (DF) forest in BC (BC_DF). Canopy heights ranged from 11 m (SK_BS) to 33 m (BC_DF) and ages varied from 30 (ON_WPP74) to 120 years (BC_DF; Table 1). The sites were chosen primarily for their unique species characteristics, geographic location, and availability of 2004 datasets.

2.2. *Flux measurements*

Each site was equipped with a tower-mounted eddy covariance (EC) system which consisted of one infrared gas analyzer (IRGA), either a LI-7000 or LI-6262 (close path IRGA, Li-COR, Lincoln, Nebraska) or a LI-7500 (open path) and a 3-D sonic anemometer, either a CSAT3 [Campbell Scientific Canada (CSC), Edmonton, Alberta] or a Gill R3 (Gill Instruments, Ltd., Hamsphire, UK; Table 1), and a fine-wire thermocouple (CSC). The closed-path IRGA's (LI-6262 or LI-7000) were enclosed in a thermostatically controlled housing painted in white minimizing the temperature effects on the measurements. Air sampled within 30 cm of the sonic array was pulled down a heated tube 4-m long to the IRGA at 10–20 L min^{-1} for fast analysis. Open-path IRGA's were mounted within 30 cm of the sonic array downwind from the anemometer. For additional information on tower and equipment set-up, sensor calibration, and maintenance schedules for all FCRN EC-towers refer to the "*FCRN Measurement Protocols*, *Working Draft*, *v. 1.3*" available on the internet (Fluxnet-Canada Network Management Office, 2003) or Coursolle et al. (2006; Table 1).

Net CO_2 and H_2O fluxes were calculated from the mean covariance between the vertical wind speed and either the CO_2 or H_2O mixing ratios for 30-min averaging times; the density measurements from the open-path IRGA's were converted to mixing ratios, closed-path IRGA's registered their results directly into mixing ratios. A co-ordinate rotation of wind vectors was used in the calculation of fluxes following procedures described in Tanner and Thurtell (1969). NEE (μmol CO_2 m^{-2} s^{-1}) was calculated based on

$$\mathrm{NEE} = F_c + S, \tag{4}$$

where F_c is the above canopy CO_2 flux and S is the CO_2 stored in the air column beneath the EC sensors (both in μmol CO_2 m^{-2} s^{-1}). Negative NEE measurements (= NEP) indicate a C sink (C uptake by the vegetation is active), otherwise positive NEE indicates a C source (C is released by the system). The storage term (S) was calculated either (i) as the difference between the subsequent and the previous half-hour CO_2 concentration, multiplied by the height of the air column beneath the EC sensor (one-level approach, Baldocchi et al., 1997), or (ii) by integrating one-level calculations made at several points along the tower (a minimum of 4–6 points). Generally, the

storage term was calculated by the multiple-level approach whenever the CO_2 concentration profile was available (e.g., NB_BF, ON-WPP39, ON_WPP74, and BC_DF); otherwise the one-level approach was used (e.g., QC_OBS, ON_OMW, SK_OA, and SK_OBS).

2.3. Meteorological measurements

PAR was measured at the height of flux measurement with a LI-189 or LI-190 quantum sensor (LI-COR) or a BF-2 or BF-3 sunshine sensor (Delta-T Instruments, Cambridge, UK) which permitted separation of global PAR into its two components (i.e., direct and diffuse PAR; Table 2). Air temperature and relative humidity were measured with an HMP45C T-RH probe (CSC) also set at the height of flux measurement. The soil temperatures were measured with 107 thermisters (CSC) set at soil depths of 2, 5, 10, 20, 50, and 100 cm from the surface (Table 2). The soil moisture profile was measured with CS616 or CS615 soil moisture reflectometers (CSC) installed at 5, 10, 20, 50 cm from the surface.

2.4. Model description

2.4.1. Selection of an appropriate light response model and its refinement

To select an equation which can best represent the mean pattern of NEP as a function of PAR, an inter-equation comparison of the three PAR-based equations introduced earlier was carried out. Preliminary fitting of the three equations [Eqs. (1)–(3)] to a 36-day time series showed comparable results ($r^2 = 0.72$–0.73 for all three fits). **Model 1** [Landsberg's equation; Eq. (3)] obtained slightly lower r^2's when PAR was above 1000 $\mu mol\,m^{-2}\,s^{-1}$ and slightly higher r^2's when PAR was between 300 and 1000 $\mu mol\,m^{-2}\,s^{-1}$. Given the minor improvement with Landsberg's equation, we decided to adopt Landsberg's equation as the core equation in our gap-filling approach. **Model 1** is central to the development of **Models 2** and **3**, introduced in Section 2.4.2.

Instead of using global PAR directly (as it is done in **Model 1**), global PAR is divided into its two components and redistributed in the canopy according to available direct and diffuse PAR (both functions of sun-earth geometry and sky cloudiness). Modification of light interception in **Model 1** by incorporating a representation of sunlit and shaded leaves and associated absorption rates (i.e., the two-big leaf model concept) yield **Model 2**. **Model 3** is based on subdividing the canopy description in **Model 2** into multiple layers. Model development is approached in this stepwise manner so that an evaluation of the contribution of individual enhancements to overall improvement of model predictions may be quantified. Description of the individual models follows below.

2.4.2. Model enhancements

2.4.2.1. ***Model 2**: two-big-leaf extension of **Model 1***. A two-big-leaf formulation following De Pury and Farquhar (1997) was incorporated into **Model 1** (Landsberg's equation) resulting in **Model 2**. The governing equations of **Model 2** are as follows:

$$\mathrm{NEP} = \mathrm{NEP}_{\max}\mathrm{LAI}[1 - f_{\mathrm{sun}}\exp\{-\alpha(\mathrm{PAR}_{\mathrm{sun}} - \Gamma)\} - f_{\mathrm{shade}}\exp\{-\alpha(\mathrm{PAR}_{\mathrm{shade}} - \Gamma)\}], \quad (5)$$

where f_{sun} and f_{shade} represent the sunlit and shaded leaf portions of the canopy, i.e.,

$$f_{\mathrm{sun}} = 1 - \exp(-k_{\mathrm{d}}\mathrm{LAI}) \quad (6)$$

$$f_{\mathrm{shade}} = 1 - f_{\mathrm{sun}} \quad (7)$$

and $\mathrm{PAR}_{\mathrm{sun}}$ is the PAR absorbed by sunlit leaves and determined by

Table 2 – Growing season means for selected meteorological variables for the eight forest sites

Variables[a]	NB_BF	QC_OBS	ON_WPP39	ON_WPP74	ON_OMW	SK_OA	SK_OBS	BC_DF
DailytPAR	18,976	16,467	20,682	17,158	17,978	17,972	17,462	17,004
tPAR	656	607	741	738	617	583	581	613
$\mathrm{DailyPAR_d}$	14459	7439	n/a	n/a	8253	n/a	n/a	9896
$\mathrm{PAR_d}$	378	275	n/a	n/a	285	n/a	n/a	369
$\mathrm{DailyPAR_{df}}$	7610	9028	n/a	n/a	9725	n/a	n/a	7108
$\mathrm{PAR_{df}}$	278	332	n/a	n/a	332	n/a	n/a	244
Rain	346	n/a	407	n/a	428	366	523	584
WindSP	2.7	2.5	2.1	1.4	3.6	1.9	3.3	0.79
T_a	11.5	12.5	15.9	16.4	7.5	11.93	11.4	12.5
RH	73	74	84	78	73	72	67	74
T_s (2)	10.6	10.4	15.3	16.7	10.4	11.02	7.5	11.5
T_s (5)	9.9	9.3	15.2	16	9.8	11	7	11.1
T_s (10)	10	8.7	15.4	15.3	9	10.8	6	12
T_s (20)	9.2	9.1	14.7	15.5	8.5	10.4	6.1	11.3
T_s (50)	8	7.4	13.7	13.4	7.9	9.5	5.5	11.1
T_s (100)	n/a	6.5	12.2	n/a	7.1	n/a	5.1	9.4
Date_period	100–305	150–290	120–300	120–300	120–300	160–267	140–290	82–308

[a] Prefix Dailyt: daily total; t: half-hourly total; Dailyd: daily direct; Dailydf: daily diffuse; T_a: air temperature; RH: relative humidity; T_s: soil temperature, the values in brackets provide the level (in cm from the surface) that the temperatures were taken; Date_period: day of year (DOY) data were obtained; n/a: measurements were not available at the time of writing.

$$\mathrm{PAR_{sun}} = \mathrm{PAR_d}(1-\sigma)[1-\exp(-k_b \mathrm{LAI})] + \frac{\mathrm{PAR_{df}}(1-\rho_{cd})\{1-\exp[-(k'_d+k_d)\mathrm{LAI}]\}\cdot k'_d}{k'_d+k_d} + \mathrm{PAR_d}\left[\frac{(1-\rho_{cb})\{1-\exp[-(k'_b+k_b)\mathrm{LAI}]\}\cdot k'_b}{k'_b+k_b} - \frac{(1-\sigma)}{2}\cdot[1-\exp(-2k_b\mathrm{LAI})]\right] \quad (8)$$

where k_b (a function of solar position) and k_d are the extinction coefficients for direct and diffuse PAR ($\mathrm{PAR_d}$ and $\mathrm{PAR_{df}}$), respectively, σ is the scattering fraction of PAR which is assumed constant (0.15; De Pury and Farquhar, 1997), k'_b and k'_d are modified extinction coefficients to account for the scattering of $\mathrm{PAR_d}$ and $\mathrm{PAR_{df}}$ by leaves, and $\mathrm{PAR_{shade}}$ is the PAR absorbed by shade leaves, i.e.,

$$\mathrm{PAR_{shade}} = \mathrm{PAR_c} - \mathrm{PAR_{sun}} \quad (9)$$

where

$$\mathrm{PAR_c} = \int_0^{\mathrm{LAI}} \mathrm{PAR}\cdot d\lambda = (1-\rho_{cb})\mathrm{PAR_d}[1-\exp(-k'_b\mathrm{LAI})] + (1-\rho_{cd})\mathrm{PAR_{df}}[1-\exp(-k'_d\mathrm{LAI})] \quad (10)$$

is the total PAR absorbed by the canopy, LAI is the total leaf area index ($\mathrm{m^2\,leaf\,m^{-2}}$ ground), and ρ_{cb} and ρ_{cd} are canopy reflectivities for $\mathrm{PAR_d}$ and $\mathrm{PAR_{df}}$, respectively.

2.4.2.2. ***Model 3**: multiple canopy-layer light interception extension of **Model 2***. The basic equations in **Model 3** are the same as those in **Model 2**, except in **Model 3** the canopy is subdivided into several layers. Therefore, f_{sun}, f_{shade}, $\mathrm{PAR_{sun}}$ and $\mathrm{PAR_{shade}}$ are represented as arrays, where each element of the array is a variable value for a specific canopy layer. The total leaf area (LAI) is equally partitioned among the canopy layers and as result NEP is redefined as

$$\mathrm{NEP} = \sum_{i=1}^{n}\mathrm{NEP}[i], \quad (11)$$

where i represents the ith canopy layer and n is the total number of canopy layers implemented. A generalized form of Landsberg's equation (**Model 1**) for a multiple-layer canopy becomes

$$\mathrm{NEP}[i] = \frac{\mathrm{NEP_{max}}\cdot\mathrm{LAI}}{n}\{1-f_{sun}[i]\cdot\exp[-\alpha(\mathrm{PAR_{sun}}[i]-\Gamma)] - f_{shade}[i]\cdot\exp[-\alpha(\mathrm{PAR_{shade}}[i]-\Gamma)]\}. \quad (12)$$

2.5. Model performance criteria

To evaluate the performance of the various models, relative root mean square error (RRMSE) is calculated, i.e.,

$$\mathrm{RRMSE} = \frac{100}{\overline{O}}\sqrt{\frac{1}{n}\sum_{j=1}^{n}(P_j-O_j)^2}, \quad (13)$$

where O_j, P_j, and n are the NEP observation value, NEP modelled value, and number of observations, respectively. $\overline{O}$ is the daily average of NEP observations. Relative error (RE) and modelling efficiency (ME) are also used as criteria to evaluate model performance, i.e.,

$$\mathrm{RE} = \frac{100}{\overline{O}}\cdot\frac{\sum_{j=1}^{n}(P_j-O_j)}{n}, \text{ and} \quad (14)$$

$$\mathrm{ME} = 1-\frac{\sum_{j=1}^{n}(P_j-O_j)^2}{\sum_{j=1}^{n}(|P'_j|-|O'_j|)^2}, \quad (15)$$

where $P'_j = P_j - \overline{O}$; and $O'_j = O_j - \overline{O}$ (Leuning et al., 1998; Willmott, 1981). Modelling efficiency ME ranges from [0,1] as agreement between predicted and observation values varies from absolutely no agreement to perfect agreement. Because ME is undefined when the denominator approaches zero (Figuerola and Mazzeo, 1997) the two other criteria are included to give an overall assessment of model performance across the model's solution space.

2.6. Data analysis software

TableCurve 2D™ v. 5.1 (SYSTAT Software Inc., CA, USA) is used to fit the single-variable equations relating NEP as a function of PAR [Eqs. (1)–(3)] to growing-season NEP measurements taken over the eight FCRN sites. **Models 2** and **3** (Section 2.4.2) because of their added complexity (i.e., greater number of variables and parameters) are fitted within the ModelMaker™ v. 3.0 modelling environment (Cherwell Scientific Company, Ltd., CA, USA). To investigate model performance of **Models 1–3**, the models are applied to a sub-sample dataset from NB_BF spanning nine days (day of year, DOY, 182–190). To get the best possible fit, model parameters for the three models are re-optimized for the 9-day period.

2.7. Model parameterization and optimization

Iterative numerical methods, such as Levenberg–Marquardt and Simplex method, are frequently used in non-linear model parameterization. This is accomplished by minimizing the difference between the model's results and target data (observations), provided in terms of the weighted sum of squares and expressed as:

$$\chi^2 = \sum\frac{(P_j-O_j)^2}{\mathrm{Er}^2}, \quad (16)$$

where O_j is the target value, P_j the calculated value, Er the uncertainty associated with the data values predetermined by the user, and j represents a specified target data-versus-prediction data pair.

3. Results and discussion

3.1. Determination of parameter-value ranges

Older WP growing in Ontario (ON_WPP39) had the highest light compensation point (Γ; 191.5 μmol PAR $\mathrm{m^{-2}\,s^{-1}}$)

Table 3 – Parameter and regression coefficient values determined by fitting Model 1 (Landsberg's equation) to NEP data for the 2004 growing season for eight forest sites

Model	Parameter	NB_BF	QC_OBS	ON_WPP39	ON_WPP74	ON_OMW	SK_OA	SK_OBS	BC_DF
$NEP = NEP_{max}$ $(1 - \exp^{-\alpha(PAR - \Gamma)})$	NEP_{max}	11.75	4.75	13.62	7.53	10.76	15.31	6.96	12.24
	α	0.00183	0.00420	0.00164	0.00320	0.00242	0.00190	0.00240	0.00460
	Γ	88.77	91.90	191.53	119.41	127.89	133.16	148.61	98.93
	r^2	0.67	0.41	0.75	0.65	0.57	0.82	0.75	0.69
	F	7795.16	1514.06	7804.48	1290.66	2295.39	8505	6279.41	5610.56
	R_d	2.07	2.24	5.03	3.50	3.90	4.41	2.98	7.05

NEP values associated with friction velocities (u^*) < 0.25 were excluded from the analysis. NEP is the net ecosystem productivity (in $\mu mol\ CO_2\ m^{-2}\ s^{-1}$), NEP_{max} the maximum NEP at optimal growing conditions, α is a shape factor [$mol\ CO_2\ (mol\ PAR)^{-1}$], and Γ the light compensation point (in $\mu mol\ PAR\ m^{-2}\ s^{-1}$), r^2 the coefficient of determination, F the ratio of mean model variation to mean residual variation, R_d the ecosystem respiration (in $\mu mol\ CO_2\ m^{-2}\ s^{-1}$). NB_BF (balsam fir site in New Brunswick), QC_OBS (old black spruce site in Quebec), ON_WPP39 (white pine plantation in Ontario; stand initiation, 1939), ON_WPP74 (white pine plantation in Ontario; stand initiation, 1974), ON_OMW (old mixedwood site in Ontario), SK_OA (old aspen site in Saskatchewan), SK_OBS (old black spruce site in Saskatchewan), and BC_DF (Douglas fir site in British Columbia).

of the species considered, followed by BS in SK (148.6 $\mu mol\ PAR\ m^{-2}\ s^{-1}$; SK_OBS); BF in NB (NB_BF) had the lowest value at 88.8 $\mu mol\ PAR\ m^{-2}\ s^{-1}$, followed by BS in QC (91.9 $\mu mol\ PAR\ m^{-2}\ s^{-1}$; QC_OBS). Regression statistics associated with fitting **Model 1** to the 2004 (growing-season) NEP data for the eight FCRN-sites appear in Table 3.

Among the species considered, OA (from the SK_OA site) had the highest NEP_{max} at 15.3 $\mu mol\ CO_2\ m^{-2}\ s^{-1}$, while BS (from the QC_OBS site) had the lowest at 4.8 $\mu mol\ CO_2\ m^{-2}\ s^{-1}$ (Table 3). NEP_{max} varied with species and, thus, with location. For example, NEP_{max} measured for BS growing at the QC_OBS and SK_OBS sites varied by 38% (the BS in SK had the higher NEP_{max} at 7.0 $\mu mol\ CO_2\ m^{-2}\ s^{-1}$), while NEP_{max} for DF growing in BC and BF in NB varied by about 4% (with NEP_{max} greatest for DF at 12.2 $\mu mol\ CO_2\ m^{-2}\ s^{-1}$). In contrast, NEP_{max} between WP plantations in Ontario (i.e., ON_WPP39 and ON_WPP74) was in between with ~30% variation. The storage term in the calculation of NEP accounted for <12% of NEP_{max} for all sites considered; the storage term at the NB_BF site accounted for about 4.4% of NEP_{max}.

Parameter α varied from site to site ranging from 0.0016 to 0.0046 $mol\ CO_2\ (mol\ PAR)^{-1}$. The mean value for the eight sites was 0.0028 $mol\ CO_2\ (mol\ PAR)^{-1}$. Nighttime ecosystem respiration (R_d; Table 3) in DF in BC was the highest at 7.1 $\mu mol\ CO_2\ m^{-2}\ s^{-1}$, followed by WP at the ON_WPP39 site at 5.0 $\mu mol\ CO_2\ m^{-2}\ s^{-1}$. Respiration in BF at the NB_BF site was the lowest at 2.1 $\mu mol\ CO_2\ m^{-2}\ s^{-1}$, while the OBS site in QC (QC_OBS) was next at 2.2 $\mu mol\ CO_2\ m^{-2}\ s^{-1}$.

This initial work using the data from the different sites provided a basis for determining the ranges of equation parameter values across species, environmental controls, and geographic locations (Table 3). These ranges defined the constraints on values used during model parameterization of **Models 2** and **3**. The lower and upper bounds of the value ranges for the four main parameter groups were set as follow: (i) Γ, from 44.4 (taken as 50% of 88.8) to 286.75 (150% of 191.5), (ii) NEP_{max}, from 2.4 (4.8 × 50%) to 23 (15.3 × 150%), (iii) α, from 0.0008 to 0.0042, and (iv) R_d, from 1.1 $\mu mol\ CO_2\ m^{-2}\ s^{-1}$ (2.1 × 50%) to 10.0 $\mu mol\ CO_2\ m^{-2}\ s^{-1}$ (7.1 × 150%).

Although **Model 1** provided more than adequate fit in most instances (Table 3), it only provided an averaged expression of NEP as a function of PAR, and accordingly did not address the day-to-day fluctuations in NEP. In general, deviation from the calculated mean (from **Model 1** predictions) increased with an increase in PAR except for ON_WPP74. For most sites considered when PAR was >500 $\mu mol\ PAR\ m^{-2}\ s^{-1}$, the deviation (±) from the mean increased by 50–100%. For comparison purposes, the BC_DF site had the largest deviation, while OBS from both SK and QC (SK_OBS and QC_OBS) had the least deviation. Residuals from individual prediction-to-measurement comparisons were as high as 300%. The large deviations suggested that significant bias could be generated with **Model 1**, in prediction of individual data points.

3.2. *2004 9-day sub-dataset from the NB_BF site*

3.2.1. *Prevailing weather conditions*

Fig. 2 provides basic weather conditions such as air and soil temperature, relative humidity, and PAR over the 9-day period (DOY = 182–190) for the NB_BF site. The average temperature for the period was 15.7 °C, with the highest temperature at 25.7 °C and lowest at 8.9 °C (Table 4). The large temperature variation provided a reasonable measure of the influence of temperature on NEP, although temperature was not specifically addressed in the models. Soil temperature fluctuations were smaller and varied from 11.2 to 15.2 °C with an average of 13.2 °C. The relative humidity varied from 26.5% to 98.0%, and among the days considered two were especially very sunny and dry, namely, DOY 183 and 189. The daytime half-hourly mean for global PAR was 503.1 $\mu mol\ PAR\ m^{-2}\ s^{-1}$, with a peak value of 1612.0 $\mu mol\ PAR\ m^{-2}\ s^{-1}$ (Table 4). The mean daytime global PAR was 15.075 $mol\ PAR\ m^{-2}\ d^{-1}$. Of the total mean daytime PAR, the diffuse component was 7.694 $\mu mol\ PAR\ m^{-2}\ d^{-1}$ and the direct component was 7.364 $\mu mol\ PAR\ m^{-2}\ d^{-1}$, leading to a mean diffusion fraction of 0.51.

3.2.2. ***Model 1** performance*

A reasonable agreement was obtained with **Model 1** producing a NEP_{max} of 12.2 $\mu mol\ CO_2\ m^{-2}\ s^{-1}$. The NEP_{max} was very close to the NEP_{max} obtained for the 2004 growing season (i.e., 11.8 $\mu mol\ CO_2\ m^{-2}\ s^{-1}$; Table 3); Γ was 82.7 $\mu mol\ m^{-2}\ s^{-1}$, slightly lower than the value for the growing season (88.8 $\mu mol\ CO_2\ m^{-2}\ s^{-1}$); and α was 0.00323 $mol\ CO_2\ (mol\ PAR)^{-1}$ compared with the growing-

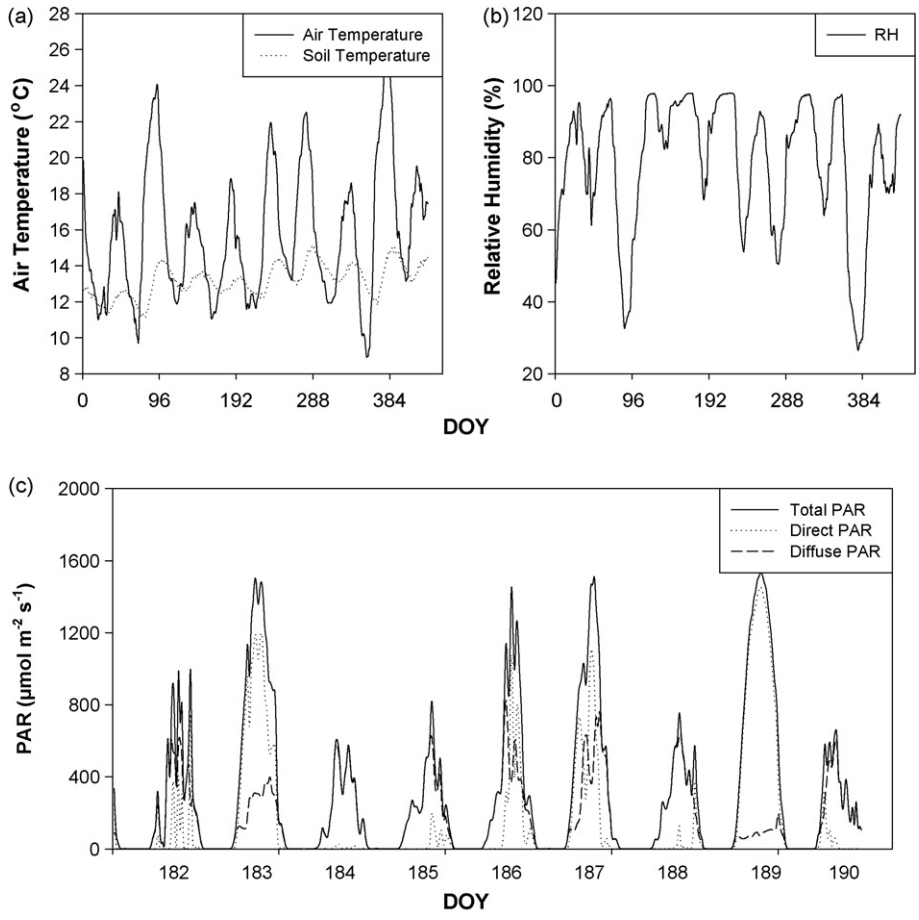

Fig. 2 – Nine-day time series (DOY = 182–190, 2004) of air and soil temperature, relative humidity (a and b), and PAR (c) for the NB_BF site. Total (global) PAR is sub-divided into its two components, direct and diffuse PAR.

season value of 0.00183 mol CO_2 (molPAR)$^{-1}$. The r^2 from fitting **Model 1** to the data was 0.63, slightly lower than the performance obtained for the growing season (with an $r^2 = 0.67$). Fig. 3a shows that **Model 1** predictions of NEP for DOY 183 and 189 were generally poor. The model underestimated the peak values for both of those two days and overestimated the NEP values for the rest of the day. Residuals of NEP (i.e., modelled–observed values) are plotted as functions of total (global), direct, and diffuse PAR (Fig. 4b–d). Although the residuals between **Model 1** predictions and observations for the 9-day period plotted with total PAR (Fig. 3a) is randomly distributed (Fig. 3b), an apparent linear relationship with direct PAR (Fig. 3c) and diffuse PAR (Fig. 3d) suggest greater explanation may be obtained with **Model 1** by decomposing total PAR into its two components and redistributing total PAR in the canopy accordingly. In general, **Model 1** performed well when the proportion of diffuse PAR was >0.5, but performed poorly when that proportion was <0.5 (Figs. 3 and 4). This discrepancy is most likely related to the fact that **Model 1** was parameterized with data that contained a larger proportion of cloudy

Table 4 – Meteorological values for the 9-day sub-sampling period (DOY = 182–190)

	NEP	T_a	RH	T_s	SM	tPAR	PAR_{df}	fd
Mean	2.64	15.73	78.67	13.20	0.09	503.14	256.77	0.45
Median	0.31	15.09	83.7	13.22	0.09	354.16	220.88	0.33
Standard deviation	7.38	3.65	18.22	0.89	0.00	26.49	11.66	0.43
Range	42.04	16.83	71.54	4.013	0.02	1600.42	821.62	1.00
Minimum	−12.85	8.91	26.46	11.15	0.08	11.54	10.28	0
Maximum	29.19	25.74	98	15.16	0.09	1611.96	831.9	1.00

Averages are given as half-hourly values. NEP measurements (filtered with $u^* > 0.25$; in μmol CO_2 m^{-2} s^{-1}), T_a is air temperature (°C), RH the relative humidity (%), T_s the soil temperature at 5 cm from the surface (°C), SM the soil moisture at 5 cm from the surface (% by volume), tPAR total PAR (μmol m^{-2} s^{-1}), and PAR_{df} diffuse PAR and fd is diffusion fraction of PAR.

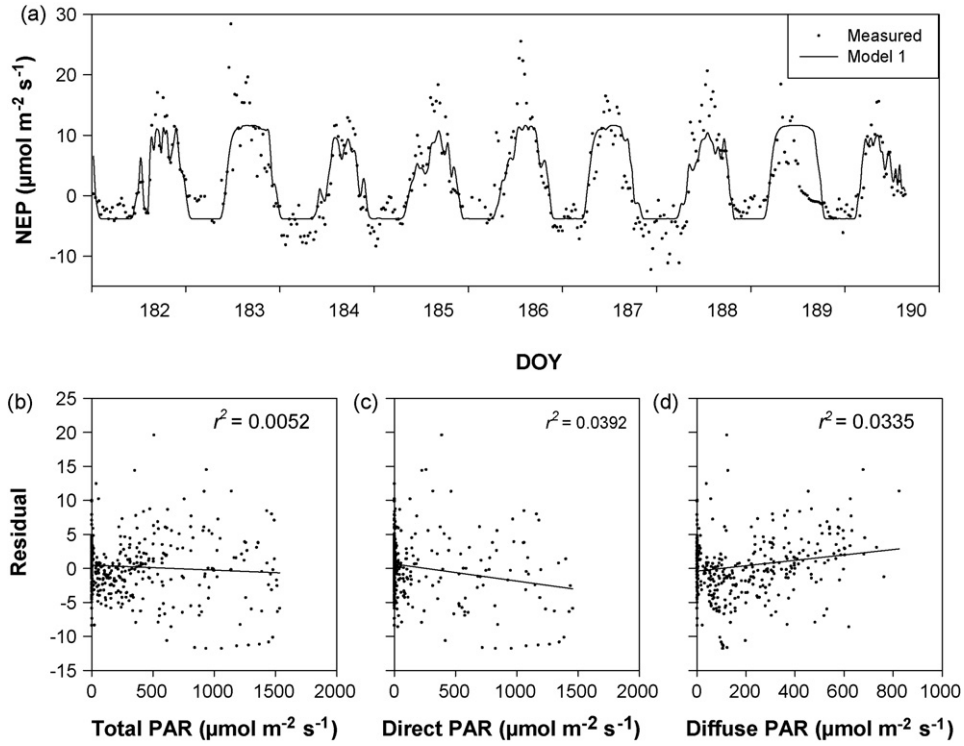

Fig. 3 – Predicted (line) and observed values (close symbols) of NEP for the 9-day period (DOY = 182–190, 2004). Model predictions in (a) are based on the application of Model 1. Plotted in figures b–d are the prediction-to-observation residuals as functions of total (b), direct (c), and diffuse PAR (d); total (global) PAR = direct PAR + diffuse PAR.

days, so when **Model 1** was used to predict NEP for cloud-free days, a systematic bias was produced.

Table 5 provides **Model 1** parameter values for model regressions applied to NEP data for each of the nine days. General relationships show that α decreases and NEP_{max} increases with increases in the proportion of diffuse PAR.

3.2.3. *Performance gains from incorporating a two-big-leaf modelling scheme*

Fig. 4 provides a comparison of observed and modelled daytime NEP values generated with **Models 1** and **2**. The level of prediction is clearly improved with **Model 2**. **Model 2** not only captures the mean NEP trend, but also significantly improves the representation of daytime trends; it generates peaked traces similar to those seen in the observed data. However, measurement-to-prediction deviation increased during the night time period in comparison to what was obtained with **Model 1**.

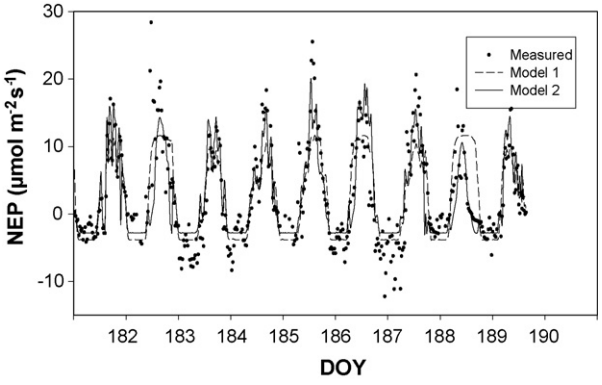

Fig. 4 – Predicted (lines) and observed values (close symbols) of NEP for the 9-day period (DOY = 182–190, 2004). Model predictions are based on the application of Model 1 (broken line) and Model 2 (solid line).

A close inspection of **Model 2** predictions on DOY 183 and 189 suggested that poor performance (especially in capturing the peak values) on those two days may have been related to other environmental controls that were not directly addressed in model formulation. The analysis found that both days had a higher proportion of direct PAR. However, the higher NEP measurements suggested a higher portion of diffuse PAR than what was actually measured. The 9-day mean ME (Fig. 5a) of **Model 2** was 3.9% higher than that of **Model 1**, indicating a slight improvement from **Model 1**.

3.2.4. *Canopy stratification and its influence on model performance*

Fig. 6 provides a model sensitivity test with **Model 3** to determine the number of canopy layers (n) the canopy can be sub-divided (LAI redistributed) for best overall explanation of light interception and reduced computational effort. From this test, four canopy layers were determined to provide the best model performance using equation-parameter values generated with fitting **Model 2** to the 9-day dataset. Beyond four layers (and greater model complexity), model calculations were no better than what was obtained with a four canopy

Table 5 – Parameter values associated with fitting Model 1 to daily NEP values

Parameters	DOY								
	182	183	184	185	186	187	188	189	190
fd	0.865234	0.440703	0.97691	0.896407	0.751431	0.631518	0.888361	0.225365	0.889469
α	0.00129	0.00475	0.001946	0.001447	0.001802	0.001324	0.001724	0.00336	0.002058
Γ	72.264	74.66	132.047	108.037	79.36	206	94.7189	280.202	89.604
NEP_{max}	21.231	12.032	17.3794	26.0351	19.51	15.7847	24.638	21.0726	14.3936

DOY: day of year; fd is the fraction of diffuse PAR to total PAR (in $\mu mol\,m^{-2}\,s^{-1}$), NEP_{max} the maximum NEP at optimal growing conditions (in $\mu mol\,CO_2\,m^{-2}\,s^{-1}$), α the shape factor [$mol\,CO_2\,(mol\,PAR)^{-1}$], and Γ is the light compensation point ($\mu mol\,PAR\,m^{-2}\,s^{-1}$).

layer model (RRMSE ~ 47%; Fig. 6). The four canopy layer model provided a better representation of measured NEP values, generating an increased r^2 (0.70) and increased ME values (Fig. 5).

Fitting **Model 3** to the 9-day dataset showed that Landsberg's equation can be greatly improved by a reformulation of the light interception term by addressing (i) canopy light variations associated with multiple scattering and

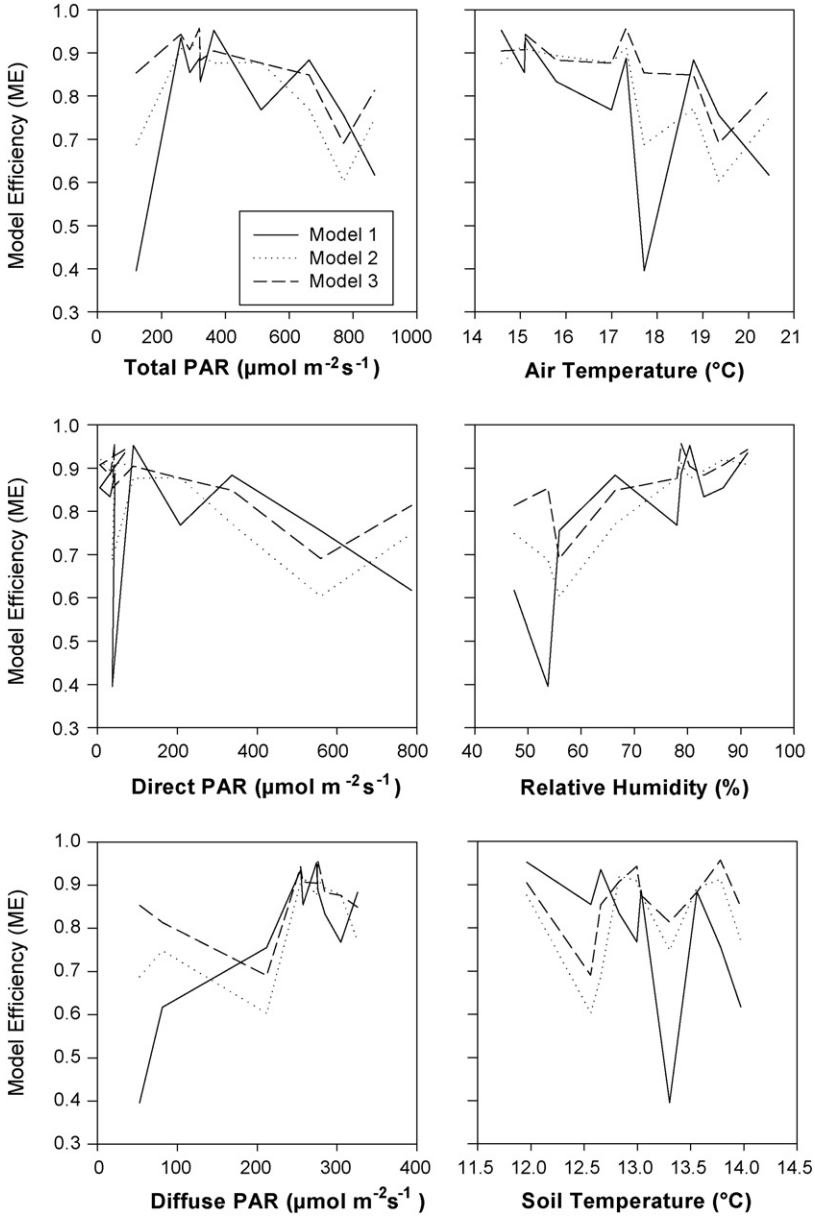

Fig. 5 – Modelling efficiency (ME) vs. total PAR (a), air temperature (b), direct PAR (c), relative humidity (d), diffuse PAR (e), and soil temperature (f). Meteorological and ME values are expressed as daily means.

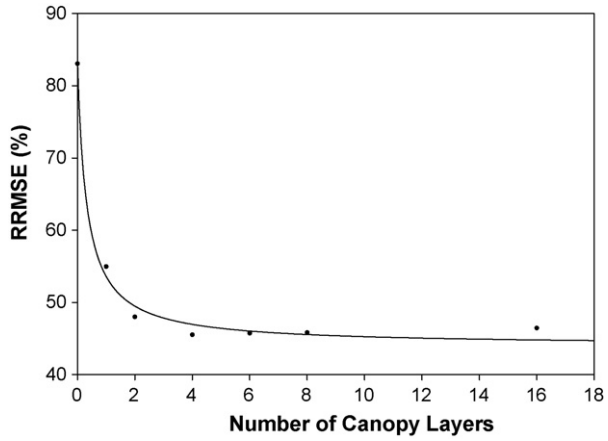

Fig. 6 – Model 3 RRMSE (in %) vs. number of canopy layers implemented.

reflections, and (ii) response differences in shaded and sunlit leaves in the canopy. As De Pury and Farquhar (1997) pointed out, a single big leaf model may lead to misinterpretations of canopy dynamics concerning known behaviour of photosynthesis because radiation attenuation and related re-distribution of light in the canopy is not directly addressed (Monsi and Saeki, 1953; Warren, 1960; de Wit, 1965; Cowan, 1968; Ross, 1975; Mäkelä, 1986; Goudriaan and Van Laar, 1994). As shown in Fig. 7, **Model 3** greatly reduces measurement-to-prediction deviations, although nighttime ecosystem respiration remains problematic. The r^2 was increased from 0.63 obtained with **Model 1**, to 0.66 with **Model 2**, to 0.70 with **Model 3**. Optimized model parameters for the three models appear in Table 6. Modelling efficiency (ME) values across PAR values were generally more uniform with **Model 3**; **Model 1** provided greater variability (Fig. 5). The ME values of **Model 3** were generally >10% than ME-values generated with **Model 2**. ME values of **Model 3** were consistently greater than those for **Models 1** and **2** with respect to air and soil temperature, and relative humidity. ME values with **Model 3** showed near-linear directional tendencies with relative humidity and air temperature (Fig. 5b and d). Low ME values indicated the range of air temperature and relative humidity values that the model performed poorly; this information was crucial to defining the role air temperature and relative humidity played in controlling NEP. ME results for soil temperature were more difficult to interpret as there were no obvious trends.

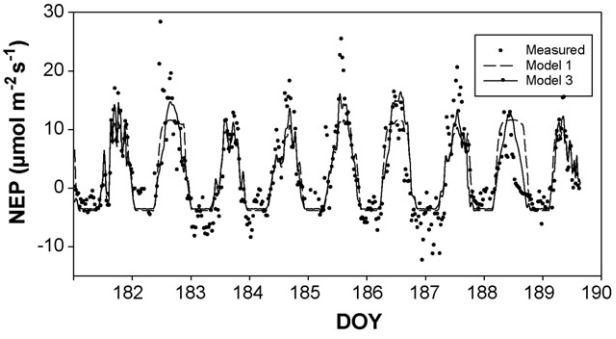

Fig. 7 – Predicted (lines) and observed values (close symbols) of NEP for the 9-day period (DOY = 182–190, 2004). Model predictions are based on the application of Model 1 (broken line) and Model 3 (solid line).

Table 6 – Equation parameter values for the 9-day sub-dataset from NB_BF

Model	α	Γ	NEP_{max}	Note
1	0.0032292	82.68	12.19	LAI = 8.4, σ = 0.15, and k_d = 0.75 for all model runs
2 and **3**	0.0049365	57.19	7.99	

NEP_{max} is the maximum NEP at optimal growing conditions (in $\mu mol\ CO_2\ m^{-2}\ s^{-1}$), α is slope of NEP as a function of photosynthetically active radiation [$mol\ CO_2\ (mol\ PAR)^{-1}$] and shape factor, and Γ the light compensation point ($\mu mol\ PAR\ m^{-2}\ s^{-1}$), σ the scattering fraction of PAR, and k_d is the extinction coefficient for diffuse PAR (De Pury and Farquhar, 1997).

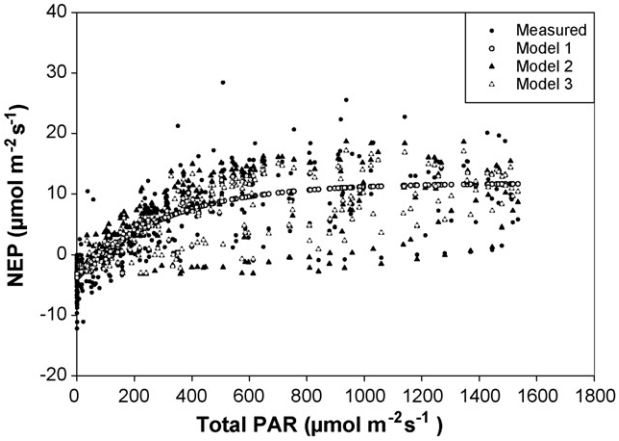

Fig. 8 – Predicted (Models 1–3) and observed NEP vs. total PAR.

In comparison to **Model 1**, **Model 3** (Fig. 7) was able to capture a greater number of the peak values in the observed data. Corrections applied to DOY 183 and 189 were offset by a slight reduction in model performance on DOY 190, 188 and 182.

3.2.5. *Overall model performance*

Fig. 8 provides a comparison of **Models 1–3** predictions against measured NEP values plotted as a function of PAR (their model parameters appear in Table 6). Clearly, **Models 2** and **3** provided a larger distribution of values, mimicking to some extent the distributional pattern observed in the real data. The lack of agreement with some observations was most likely related to the interaction of other environmental factors (e.g., air and soil temperature, soil moisture, etc.), which we planned to study and incorporate as refinements to **Model 3** in a series of additional modelling papers.

4. Conclusions

This research concluded that **Model 1** (Landsberg's equation) can represent the mean trend of NEP well for entire growing seasons, but it performs poorly in capturing day-to-day vari-

ation. Refinements to Landsberg's equation by incorporating reformulations of the light interception term by (i) partitioning global PAR into its two radiation components (direct and diffuse), (ii) treating each component according to shaded and sunlit leaf response functions (**Model 2**), and (iii) by subdividing the canopy into four canopy layers (**Model 3**) was shown to improve prediction of NEP. Reduced inter-correlated parameters in model formulation allowed the model (i) to be optimized by numerical convergence rules, and (ii) because of the model's simplicity, the model can be parameterized and applied in gap filling discontinuous time series. Disagreement between modelled NEP values and observed values are understood to be associated with environmental controlling factors other than the ones addressed in this paper, including temperature, water availability, and their interactions, which will be addressed in separate articles. The current model focuses on the light response of plants during the day and, as a result, fares poorly for nighttime conditions. Advisably, **Model 3** is designed to fill small data gaps in the daytime portion of the data stream, when fluctuations in temperature and water availability are minor. The current model provides a constant respiration term equivalent to ecosystem maintenance that will undergo further improvement in later investigations.

Acknowledgements

This paper could not have been completed without funding support from the Natural Science and Engineering Council of Canada (NSERC) and Canadian Foundation of Climate and Atmospheric Sciences (CFCAS), through the Fluxnet-Canada project. We thank the following for being able to use their FCRN field measurements in order to estimate the numerical ranges for several key model parameters described in the paper, including Hank Margolis and Carole Coursolle (QC_OBS site), Harry McCaughey (ON_OMW site), Altaf Arain (ON_WPPP sites), Alan Barr (SK_OA and SK_OBS sites), and Andy Black (BC_DF site). We are grateful for receiving logistical and financial assistance from Natural Resources Canada–Canadian Forest Service, Atlantic Forestry Centre in support of a range of field activities carried out at the NB_BF flux site.

REFERENCES

Amiro, B.D., Barr, A.G., Black, T.A., Iwashita, H., Kljun, N., McCaughey, J.H., Morgenstern, K., Murayama, S., Nesic, Z., Orchansky, A.L., Saigusa, N., 2006. Carbon, energy and water fluxes at mature and disturbed forest sites, Saskatchewan, Canada. Agric. For. Meteorol. 136 (3–4), 237–251.

Anderson, M.C., Norman, J.M., Meyers, T.P., Diak, G.R., 2000. An analytical model for estimating canopy transpiration and carbon assimilation fluxes based on canopy light-use efficiency. Agric. For. Meteorol. 101, 265–289.

Arain, M.A., Restrepo-Cope, N., 2005. Net ecosystem production in a temperature pine plantation in southeastern Canada. Agric. For. Meteorol. 128, 223–241.

Aubinet, M., Grelle, A., Ibrom, A., Rannik, U., Moncrieff, J., Foken, T., Kowalski, A.S., Martin, P.H., Berbigier, P., Bernhofer, C., Clement, R., Elbers, J., Granier, A., Grunwald, T., Morgenstern, K., Pilegaard, K., Rebmann, C., Snijders, W., Valentini, R., Vesala, T., 2000. Estimates of the annual net carbon and water exchange of forests: the EUROFLUX methodology. Adv. Ecol. Res. 30, 113–175.

Baldocchi, D., Vogel, C.A., Hall, B., 1997. Seasonal variation of carbon dioxide exchange rates above and below a boreal jack pine forest. Agric. For. Meteorol. 83, 147–170.

Bhatti, J.S., Apps, M.J., Jiang, H., 2002. Influence of nutrient, disturbances and site conditions on carbon stocks along a boreal forest transect in central Canada. Plant Soil 242, 1–14.

Bourque, C.P.-A., Lehnert, S., Xing, Z., Meng, F.-R., Swift, D.E., Cox, R.M., 2006. Site influences on net ecosystem productivity in fifteen managed balsam fir [*Abies balsamea* (L.) Mill] stands in southwest New Brunswick, Canada. In: Proceedings of International Conference on Regional Carbon Budgets, pp. 25–31.

Chen, J., Falk, M., Euskirchen, E., Paw, U.K.T., Suchanek, T., Ustin, S., Bond, B.J., Brosofske, K.D., Phillips, N., Bi, R.C., 2002. Biophysical controls of carbon flows in three successional Douglas-fir stands based on eddy-covariance measurements. Tree Physiol. 22, 169–177.

Chen, J.M., Govind, A., Sonnentag, O., Zhang, Y.Q., Barr, A., Amiro, B., 2006. Leaf area index measurements at Fluxnet Canada forest sites. Agric. For. Meteorol. 140 (1–4), 257–268.

Coursolle, C., Margolis, H.A., Barr, A.G., Black, T.A., Amiro, B.D., McCaughey, J.H., Flanagan, L.B., Lafleur, P.M., Roulet, N.T., Bourque, C.P.-A., Arain, M.A., Wofsy, S.C., Dunn, A., Morgenstern, K., Orchansky, A.L., Bernier, P.Y., Chen, J.M., Kidston, J., Saigusa, N., Hedstrom, N., 2006. Late-summer carbon fluxes from Canadian forests and peatlands along an east–west continental transect. Can. J. For. Res. 36 (3), 783–800.

Cowan, I.R., 1968. The interception and absorption of radiation in plant stands. J. Appl. Ecol. 5, 367–379.

De Pury, D.G.G., Farquhar, G.D., 1997. Simple scaling of photosynthesis from leaves to canopies without the errors of big-leaf models. Plant Cell Environ. 20, 537–557.

de Wit, C.T., 1965. Photysynthesis of leaf canopy. Agricultural Research Report No. 663. PUDOC, Wageningen.

Falge, E., Baldocchi, D., Olson, R., Anthoni, P., Aubinet, M., Bernhofer, C., Burba, G., Ceulemans, G., Clement, R., Dolman, H., Granier, A., Gross, P., Grunwald, T., Hollinger, D., Jensen, N.O., Katul, G., Keronen, P., Kowalski, A., Lai, C.T., Law, B.E., Meyers, T., Moncrieff, J., Moors, E., Munger, J.W., Pilegaard, K., Rannik, U., Rebmann, C., Suyker, A., Tenhunen, J., Tu, K., Verma, S., Vesala, T., Wilson, K., Wofsy, S., 2001a. Gap filling strategies for long term energy flux data sets. Agric. For. Meteorol. 107, 71–77.

Falge, E., Baldocchi, D., Olson, R., Anthoni, P., Aubinet, M., Bernhofer, C., Burba, G., Ceulemans, R., Clement, R., Dolman, H., Granier, A., Gross, P., Grunwald, T., Hollinger, D., Jensen, N.O., Katul, G., Keronen, P., Kowalski, A., Lai, C.T., Law, B.E., Meyers, T., Moncrieff, H., Moors, E., Munger, J.W., Pilegaard, K., Rannik, U., Rebmann, C., Suyker, A., Tenhunen, J., Tu, K., Verma, S., Vesala, T., Wilson, K., Wofsy, S., 2001b. Gap filling strategies for defensible annual sums of net ecosystem exchange. Agric. For. Meteorol. 107, 43–69.

Figuerola, P.I., Mazzeo, N.A., 1997. An analytical model for the prediction of nocturnal and dawn surface temperatures under calm, clear sky conditions. Agric. For. Meteorol. 85, 229–237.

Fluxnet-Canada Network Management Office, 2003. Fluxnet-Canada measurement protocols, Working Draft v. 1.3, http://www.fluxnet-canada.ca/pages/protocols_en/measurement%20protocols_v.1.3_background.pdf, Faculté de Foresterie et de Géomatique, Univ. Laval, Québec, QC.

Goudriaan, J., Van Laar, H.H., 1994. Radiation in crop. In: Modelling Potential Crop Growth Processes. Kluwer Academic Publisher, pp. 95–118.

Grant, R.F., Arain, M.A., Arora, V., Barr, A., Black, T.A., Chen, J., Wang, S., Yuan, F., Zhang, Y., 2005. Intercomparison of techniques to model high temperature effects on CO_2 and

energy exchange in temperate and boreal coniferous forests. Ecol. Model. 188, 217–252.
Greco, S., Baldocchi, D.D., 1996. Seasonal variations of CO_2 and water vapor exchange rates over a temperate deciduous forest. Global Change Biol. 2, 183–196.
Gu, L., Baldocchi, D., Verma, S.B., Black, T.A., Vesala, T., Falge, E.M., Dowty, P.R., 2002. Advantages of diffuse radiation for terrestrial ecosystem productivity. J. Geophys. Res. 107, 4050.
Hollinger, D.Y., Kelliher, F.M., Schulze, E.-D., Bauer, G., Arneth, A., Byers, J.N., Hunt, J.E., McSeveny, T.M., Kobak, K.I., Milukova, I., Sogatchev, A., Tatarinov, F., Varlargin, A., Ziegler, W., Vygodskaya, N.N., 1998. Forest-atmosphere carbon dioxide exchange in eastern Siberia. Agric. For. Meteorol. 90, 291–306.
Hui, D.F., Wan, S.Q., Su, B., Katul, G., Monson, R., Luo, Y.Q., 2004. Gap-filling missing data in eddy covariance measurements using multiple imputation (MI) for annual estimations. Agric. For. Meteorol. 121, 93–111.
Landsberg, J.J., 1977. Some useful equations for biological studies. Exp. Agric. 13, 272–286.
Leuning, R., Dunin, F.X., Wang, Y.P., 1998. A two-leaf model for canopy conductance, photosynthesis and partitioning of available energy. II. Comparison with measurements. Agric. For. Meteorol. 91, 113–125.
Liu, J., Chen, J.M., Cihlar, J., Park, W., 1997. A process-based boreal ecosystems productivity simulator using remote sensing inputs. Rem. Sens. Environ. 62, 158–175.
Mäkelä, A., 1986. Stand growth model based on carbon uptake and allocation in individual trees. Ecol. Model. 33, 205–229.
Mäkelä, A., Beninger, F., Hari, P., 1996. Optimal control of gas exchange during draught: theoretical analysis. Ann. Bot. 77, 461–467.
Monsi, M., Saeki, T., 1953. Über den lichtfaktor in den pflanzengesellschaften und seine bedeutung fur die stoffproduktion. Jpn. J. Bot. 14, 22–52.
Ross, J., 1975. Radiative transfer in plant communities. In: Monteith, J.L. (Ed.), Vegetation and the Atmosphere, vol. 1, Principles. Academic Press, London, pp. 13–55.
Tanner, C.B., Thurtell, G.W., 1969. Sesible Heat Flux Measurements with a Yaw Sphere and Thermometer. TR Ecom 66-G22-F. Department of Soil Science, University Wisconsin, Madison, Wisconsin.
Taylor, S.H., MacLean, D.A., 2005. Rate and causes of decline of mature and overmature balsam fir and spruce stands in New Brunswick, Canada. Can. J. For. Res. 35, 2479–2490.
Verseghy, D.L., McFarlane, N.A., Lazare, M., 1991. Class-A Canadian land surface scheme for GCMs II, vegetation model and coupled run. Int. J. Climatol. 13, 347–370.
Warren, W.J., 1960. Inclined point quadrats. New Phytol. 59, 1–8.
Willmott, C.J., 1981. On the validation of models. Phys. Geogr. 2, 184–194.